Effects of spatial detail of soil information on watershed modeling

A.X. Zhu[a,*], D. Scott Mackay[b]

[a]*Department of Geography, University of Wisconsin–Madison, 550 North Park Street, Madison, WI 53706, USA*
[b]*Department of Forest Ecology and Management and Institute of Environmental Studies, University of Wisconsin–Madison, 1630 Linden Dr., Madison, WI 53706, USA*

Abstract

The impacts of detailed and spatially continuous soil information on hydro-ecological modeling over watersheds of mesoscale size are investigated. The impacts were assessed by comparing the simulated hydro-ecological responses based on the detailed soil spatial information derived from a fuzzy logic-based inference approach with those based on the soil information derived from a conventional soil map. This study reveals that the detailed soil spatial information has impacts on the simulated hydro-ecological responses under a lumped parameter approach. Peak runoff was reduced, yielding more realistic hydrographs for forested watersheds in the area. The detailed soil spatial information strongly impacted the simulation of net photosynthesis over the period when there is a moisture stress, but negligible impacts when there is sufficient water recharge to soil profiles. Simulation of hydro-ecological responses using a distributed parameter approach is less impacted by the detailed soil spatial information. The difference in simulated net photosynthesis under the distributed approach is smaller and also only occurred during the period of moisture stress. The impacts on spatial distribution of simulated transpiration occurred mainly over south facing slopes during the period of moisture stress. © 2001 Elsevier Science B.V. All rights reserved.

Keywords: GIS; Hydro-ecological modeling; Soil mapping; Fuzzy logic; Soil landscape model

1. Introduction

Simulation of hydro-ecological responses over mesoscale watersheds requires information on the spatial distribution of soil hydraulic properties, as well as rooting depths, which affect water available for vegetation use (Burrough, 1996; Corwin, 1996; Waring and Running, 1998, pp. 50–51). Soil maps produced from conventional soil surveys are currently the major source of soil spatial information for hydro-ecological modeling of mesoscale watersheds (Lytle, 1993; Waring and Running, 1998, pp. 235–236). However, standard soil surveys were not designed to

provide the detailed (high-resolution) soil information required by this kind of environmental modeling (Band and Moore, 1995; Nielsen et al., 1996; Zhu, 1999a) due to the cartographic model and manual delineation process used in producing conventional soil maps. Soil spatial variation portrayed in conventional soil maps is often highly generalized and often discreet (Seyfried, 1998; Waring and Running, 1998, pp. 235–236; Zhu, 1997) and is incompatible with other landscape data derived from detailed digital terrain analyses and remote sensing (RS) techniques (Band and Moore, 1995; Zhu, 1997; Zhu, 1999a). This incompatibility often biases the characterization of spatial co-variation between soil spatial information and other detailed landscape data (Zhu, 2000). A more realistic characterization of spatial co-variation of

* Corresponding author. Fax: +1-608-265-3991.
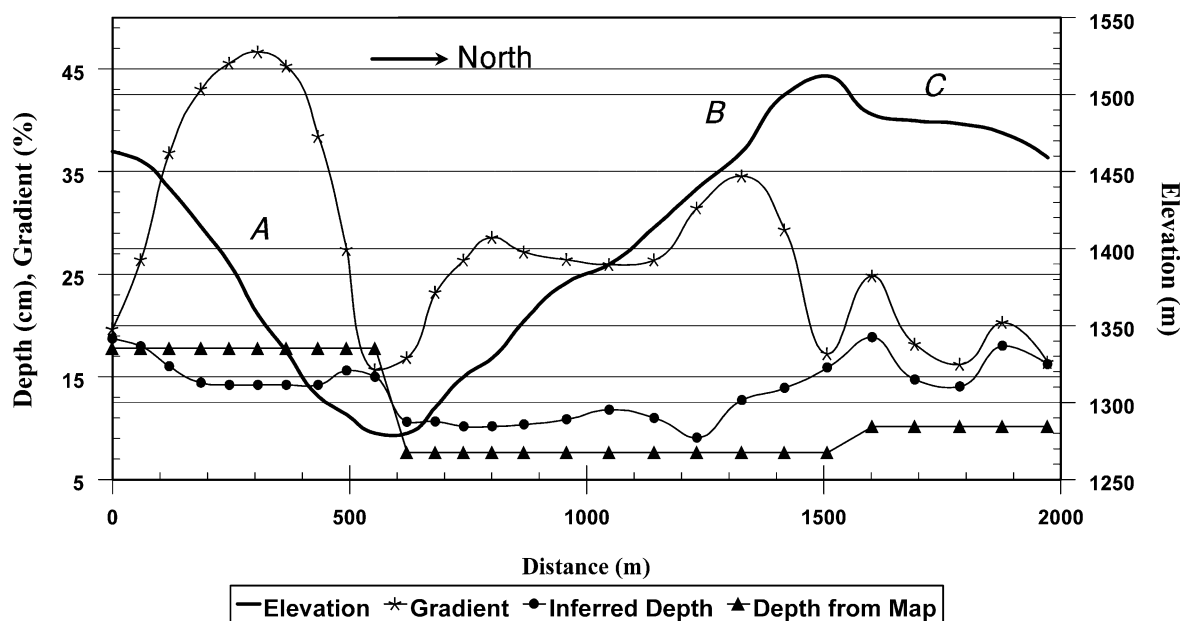 *E-mail address:* axing@geography.wisc.edu (A.X. Zhu).

Fig. 1. Co-variation of *A*-horizon depth with slope gradient and elevation along a transect in the Lubrecht area, west Montana. 'Inferred depth' is derived using the SoLIM approach while the 'depth from map' is from the conventional soil map. Figure from Zhu (2000), reproduced with permission, Water Resource Research.

model parameters is highly desirable for us to understand and model many hydro-ecological processes at the watershed scale.

Zhu and Band (1994), Zhu et al. (1996), Zhu et al. (1997), Zhu (1997), Zhu (1999b), and Zhu (2000) have developed a soil-land inference model (SoLIM) to overcome the limitations in conventional soil surveys. This approach combines the knowledge of local soil scientists with geographic information systems (GIS) techniques under fuzzy logic to map soils at a finer spatial detail and higher attribute accuracy. This detailed and spatially continuous soil information is more compatible with other landscape data derived from detailed digital terrain analyses and RS techniques (Zhu, 2000).

Zhu (2000) has demonstrated that the pattern of spatial co-variation between soil properties and other landscape parameters can be better approximated with the soil information derived from the SoLIM approach (Fig. 1). Based on the *A*-horizon depth derived from the conventional soil map the depth does not seem to relate to the slope gradient. However, with the inferred *A*-horizon depth from SoLIM, an important spatial co-variation of depth

with slope gradient was revealed. On the north-facing slope (labeled as A) the depth was negatively related to the slope gradient. On the south facing slope (labeled as B) the spatial co-variation of depth and slope gradient follows this pattern at low elevation, but this pattern of co-variation is no longer valid at high elevation. On the plateau (labeled as C), the co-variation takes a very different form. The depth is positively related to the slope gradient. It is important to know the impacts the two different characterizations of spatial co-variation will have on the simulated hydro-ecological responses at the mesoscale watershed level.

The impacts of soil spatial variability on hydro-ecological processes have been examined to some extent by several authors (Luxmoore and Sharma, 1980; Luxmoore and Sharma, 1984; Peck et al., 1977; Sharma and Luxmoore, 1979). In their examinations soil spatial variability was quantified as frequency distributions using the scaling theory (Sharma et al., 1980), and the relative importance of a range of soil properties and their frequency distributions on water balance and ecological processes were then evaluated. Scaling of soil properties by similar
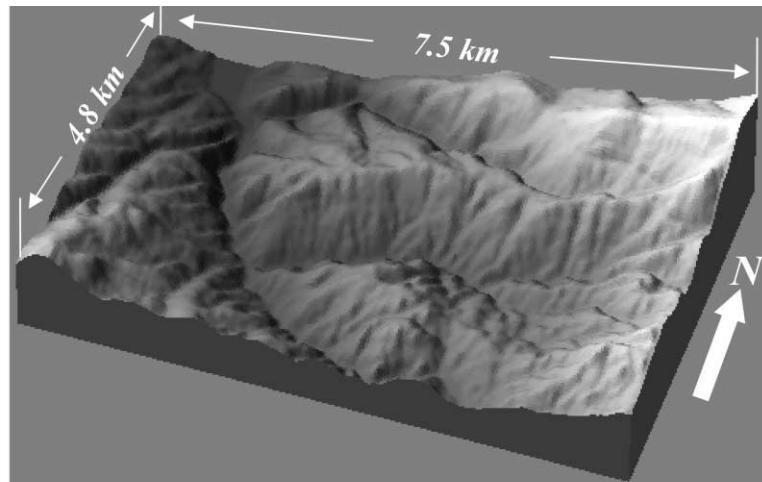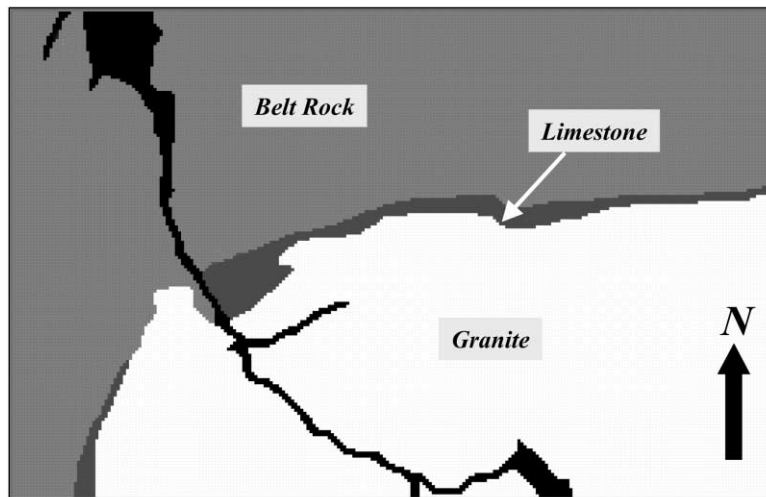
Fig. 2. The Lubrecht study area, Montana. (a) A block diagram of the digital elevation model of the area; (b) bedrock geology map (black areas are stream areas).

media criteria (Miller and Miller, 1965), on which the scaling theory is based, provided a convenient approach in studying the consequence of soil heterogeneity. But it is difficult to use scaling theory to explicitly map the spatial variability of soil properties. As a result the spatial co-variation of soil properties with other model parameters could not be quantified and the impacts of this co-variation on simulated hydro-ecological processes could not be studied.

In this paper we examine impacts of spatially explicit and detailed soil spatial information from the SoLIM approach on watershed modeling compared to watershed modeling using conventional soil maps. Specifically, we examine its impacts on the modeling of overall hydro-ecological responses over an entire area, and the modeling of spatial variation of hydro-ecological responses within the area. Since no field measured stream flow data were available, our
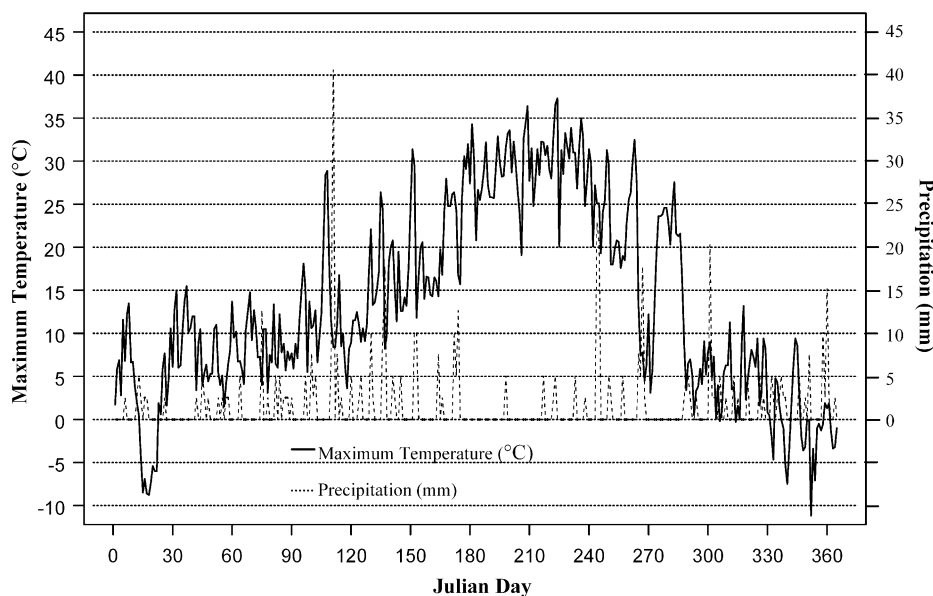
Fig. 3. Annual variation of daily maximum temperature and precipitation in the study area.

emphasis is on the differences in simulated hydro-ecological responses between two different ways of soil landscape paramization. In Section 2, we first describe the study area. This description will provide the context under which the simulated hydro-ecological responses and the impacts on these responses will be discussed and examined. The RHESSys model, which we use to simulate hydro-ecological responses at watershed level, is described in Section 2.2. This is then followed by the presentation of the two different methods of parameterizing the soil landscape. The experimental design for examining the impacts of detailed soil spatial information on watershed modeling is laid out in Section 2.4. Results of this experiment and discussion are provided in Section 3. Conclusions are made in Section 4.

2. Study area and methods

2.1. Study area

The study area is part of the Lubrecht Experimental Forest, which was established in 1937 to foster research on natural resources (Nimlos, 1986). The area is about 50 km northeast of Missoula and is in the mountainous area of western Montana with a moderate to strong relief. The area is 36 km^2 (3600 ha) in size. Elevation ranges from 1160 to 1930 m with high elevations in the east and southwest and low elevations running from southeast through northwest (Fig. 2a). The climate is considered to be semi-arid to semi-humid with hot and dry summers (Fig. 3). Ross and Hunter (1976) estimated that the mean annual precipitation for the Lubrecht area is between 50 and 76 cm. Approximately 44% of the precipitation falls during the winter (November–March) and 24% falls during the summer (June–August) (Nimlos, 1986). There is a strong contrast in terms of moisture conditions between north and south facing slopes and between low and high elevations. Slopes facing south at low elevations have poor moisture conditions while the moisture conditions on north-facing slopes at high elevations are wetter.

Most of the mountain slopes in the study area are forested, dominated by Douglas-fir (*Pseudotsuga menziesii*) with lesser amounts of western larch (*Larix occidentalis*) and ponderosa pine (*Pinus ponderosa*). Much of the timber is second growth. There have been no wild fires since 1937. Ponderosa pine forests dominate lower elevations, particularly on the south facing slopes due to high temperatures

Table 1
Soil series in the Lubrecht study area

Soil Series	Soil subgroup	Soil order
Soils on granite materials		
Ambrant	Udic Ustochrepts	Inceptisol
Elkner	Typic Cryochrepts	Inceptisol
Ovando	Typic Cryorthents	Entisol
Rochester	Typic Ustorthents	Entisol
Soils on the belt materials		
Evaro	Typic Cryochrepts	Inceptisol
Sharrott	Lithic Ustochrepts	Inceptisol
Tevis	Dystric Eutrochrepts	Inceptisol
Winkler	Udic Ustochrepts	Inceptisol
Winkler (Cool)	Udic Ustochrepts	Inceptisol
Soils on limestone materials		
Repp	Typic Ustochrepts	Inceptisol
Trapps	Typic Eutroboralfs	Alfisol
Whitore	Typic Cryochrepts	Inceptisol

and lower moisture conditions on these slopes. As elevation increases, ponderosa pine forests give way to Douglas-fir forests with a lesser amount of western larch and lodgepole pine (*Pinus contorta*). At high elevations (over 1650 m), subalpine fir (*Abies lasiocarpa*) and Engelmann-spruce (*Picea engelmannii*) replace Douglas-fir and become the dominant species.

There are three major bedrock types in the area: Belt rocks, granite, and limestone. Each bedrock type is contiguous with Belt rocks in the north, granite materials in the south and limestone in the middle (Fig. 2b). Belt rocks are the oldest rock in the area and were deposited during the Precambrian period about one billion years ago. The sediments from which they were formed were deposited in a shallow sea, subsequently buried and then metamorphosed into quartzites, argillites and siltites (Nimlos, 1986). Soils on these materials are formed from a mantle of colluvium. Soils formed from the Belt rock materials have a finer texture than soils from the other two materials.

A total of 12 soil series were found to be in the area (Table 1). Ambrant, Elkner, Ovando, and Rochester are the soil series occurring on the granite materials. Ambrant and Rochester are low elevation soil series and they often occur intermittently. Ambrant has a better-developed and deeper profile while Rochester has a poor profile development and contains a large amount of rock fragments. Rochester often occurs at the dry sites where limited moisture restricts the

development of the soil profile. Elkner is a mid to high elevation soil with a well-developed profile while Ovando is located at high elevations where cool temperatures limit the soil formation processes.

Soil series Evaro, Sharrott, Tevis, Winkler, and Winkler Cool developed on the Belt materials. Evaro is a high elevation soil with a well-developed soil profile. Sharrott and Winkler are low elevation soils that often occur intermittently on the Belt parent materials. They actually are the counter-parts of Rochester and Ambrant on belt materials. Tevis is a mid-elevation soil with a reasonably deep profile. Winkler Cool is a soil on north, northeast, and northwest facing slopes at low elevations. It has a better profile development than Winkler.

Repp, Trapps, and Whitore are limestone soils which occur as a narrow belt between the Belt soils in the Northwest and the granite soils in the southeast (Fig. 2b). Repp is the least developed soil on the limestone material. It is often found on the south and southwest facing slopes at low elevations. Whitore is the best developed soil on the limestone and is found at high elevations. Trapps is a mid-elevation soil. It also occurs on the north facing slopes at low elevations. Its profile development is between Repp and Whitore.

These 12 soil series fall into three soil orders: Alfisol, Entisol and Inceptisol (Nimlos, 1986). Alfisols are soils with leached, gray surface horizons and subsurface horizons with accumulations of illuvial clay. Entisols are weakly developed soils with very little organic-matter accumulation and no illuvial clay or sesquioxides and they are usually found on ridge crests in the study area. Inceptisols are young soils with little or no illuviated clays but brown subsoil horizons that indicate some translocations of sesquioxides. About 90% of the soils (in terms of areal extent) in the study area are Inceptisols. In general, soils on slopes with poor moisture conditions have a shallower soil profile than soils on slopes with wetter moisture conditions.

2.2. The RHESSys model

Regional Hydro-Ecological Simulation System (RHESSys) is a spatial data processing and simulation modeling system designed to scale up the spatial extent of water and carbon processes from stand

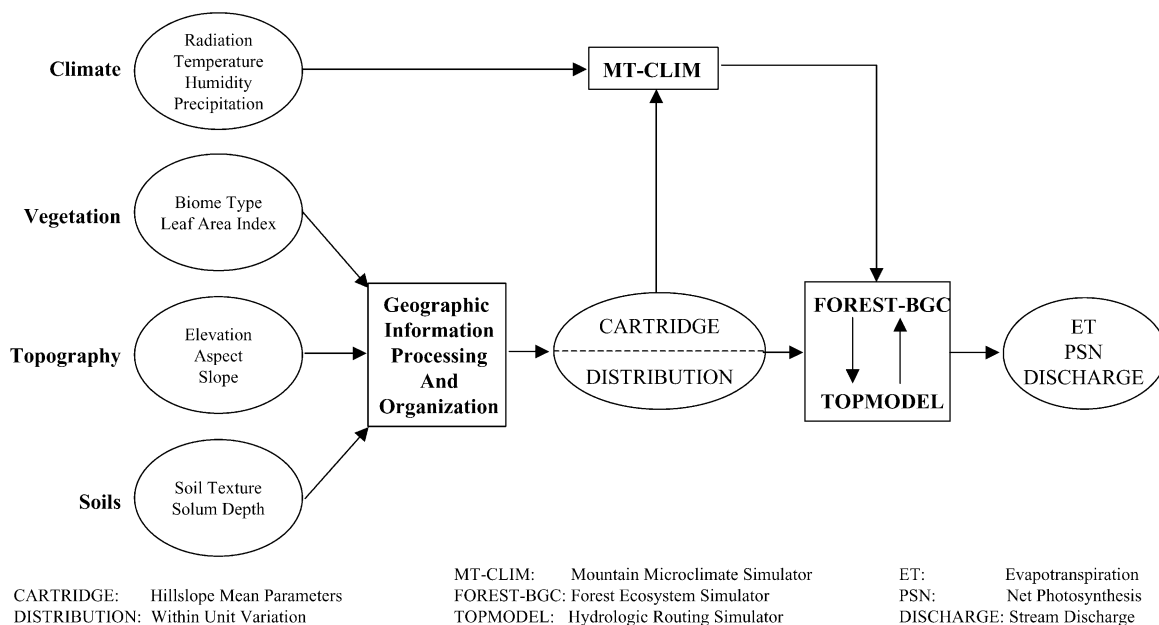REGIONAL HYDRO-ECOLOGICAL SIMULATION SYSTEM (RHESSys)

Fig. 4. Overview of RHESSys. Geographic information processing techniques are used to process and organize landscape parameters into hillslope mean parameters (landscape unit aggregation) and distribution files (within unit variability). Data in the hillslope mean parameters and distribution files are used to drive the hydro-ecological simulation models.

Table 2
RHESSys cartridge file capturing between hillslope variations (part of the cartridge file for the Lubrecht watershed. Hillslope 1 and 2 fall outside of the study area)

Hill slope ID	Aspect (°)	Elevation (m)	Gradient (°)	Leaf area[a] index (LAI)	Area (ha)	λ (m)	m	# of elevation intervals
3	276.2	1234.0	9.3	11.1	54.5	4.1	0.05	2
4	32.0	1217.0	7.2	11.5	41.2	5.6	0.05	2
5	206.2	1568.0	17.6	12.1	339.8	4.3	0.05	8
6	340.3	1449.0	11.6	12.3	309.6	3.5	0.05	8
7	261.9	1187.0	7.2	10.8	2.5	8.6	0.05	1
8	61.3	1188.0	6.9	10.9	2.7	10.3	0.05	1
9	278.0	1251.0	23.1	10.8	10.5	4.9	0.05	2
10	72.0	1216.0	18.4	12.2	5.6	11.5	0.05	2
11	248.7	1381.0	13.7	11.3	36.3	4.6	0.05	4
12	318.7	1390.0	13.5	11.9	40.4	4.5	0.05	4
13	241.7	1334.0	16.2	11.3	92.5	3.4	0.05	4
14	63.8	1365.0	14.8	12.7	153.5	4.4	0.05	4
15	221.9	1254.0	11.0	11.4	0.8	6.7	0.05	1
16	29.4	1250.0	9.6	10.9	1.1	15.2	0.05	1
17	179.9	1402.0	13.2	12.1	278.4	2.3	0.05	5
18	348.2	1377.0	14.9	13.1	139.8	1.5	0.05	4
19	185.6	1529.0	17.5	12.2	139.4	2.8	0.05	6
20	302.9	1529.0	10.5	13.2	120.3	1.6	0.05	6

[a] The LAI is all-sided.

Table 3
RHESSys distribution file (frequency file) showing the representation of parameter variation within Hillslope 3 captured by elevation bands and wetness intervals

Hillslope ID	(# of Elevation bands in the hillslope)					
3	2					

Band	Mean elevation in the band			Number of wetness intervals in the band		
1	1209.10			8		
Wetness Interval ID	Mean Wetness	Area (ha)	LAI $(m^2 m^{-2})$	Ground Coverage	K_O $(cm\ day^{-1})$	Rooting Zone Depth (cm)
2	3.72	1.08	10.70	67.5	1216.2	59.4
3	5.20	9.27	11.03	69.9	1038.1	68.0
4	7.04	11.70	11.79	75.2	836.1	75.2
5	8.85	5.76	11.70	74.6	775.4	79.6
6	10.69	1.80	11.77	75.1	914.0	69.9
7	12.69	0.27	8.94	55.0	1600.0	4.0
8	14.67	0.27	10.63	67.0	1600.0	4.0
9	17.38	9.09	8.11	49.2	1592.6	4.9

Band	Mean elevation in the band			Number of wetness intervals in the band		
2	1298.62			5		
Wetness Interval ID	Mean Wetness	Area (ha)	LAI $(m^2 m^{-2})$	Ground Coverage	K_O $(cm\ day^{-1})$	Rooting Zone Depth (cm)
2	3.96	0.09	10.63	67.0	802.4	86.5
3	5.29	4.05	12.05	77.1	568.1	101.1
4	6.91	7.20	12.41	79.6	466.1	107.6
5	8.57	2.79	12.39	79.5	485.5	107.0
6	10.69	0.09	12.18	78.0	349.9	112.2

through watersheds to regional extent (Running et al., 1989; Band et al., 1991, 1993; Nemani et al., 1993; Mackay and Band, 1997). The system is specifically designed to represent the surface soil, topographic and vegetation patterns along with certain hydro-ecological processes at the landscape level so that the necessary parameters can be realistically estimated to reproduce the dominant patterns of hydro-ecological dynamics (such as runoff generation, evapotranspiration (ET), and canopy photosynthesis) over the landscape (Band et al., 1993).

The system consists of two tightly integrated components: Geographic data processing and simulation modeling (Fig. 4). The geographical data processing component organizes landscape parameters into a multi-tiered hierarchy based on key driving environmental variables (Band et al., 1993; Mackay and Band, 1997). For example, in mountainous areas, the landscape can be first partitioned into hillslope units that reflect differences in incident short-wave radiation (the hillslope mean parameters file in Fig. 4, Table 2). Each hillslope is then partitioned into a number of elevation zones capturing within-hillslope variation in adiabatic temperature lapse rate (Lammers et al., 1997). For each of the elevation zones in a hillslope partition, wetness intervals, computed from the TOPMODEL topography-soils index (see Eq. (2) below) (Beven and Kirkby, 1979; Beven, 1986; Sivapalan et al., 1987), are used to separate areas showing different conditions of local hydrology. These within-hillslope variations in environmental conditions are represented in the distribution files (Table 3).

The simulation model combines forest ecosystem process components adapted from FOREST-BGC (Running and Coughlan, 1988; Running and Gower, 1991), a catchment hydrological model using TOPMODEL (Beven and Kirkby, 1979), and a simple, mountain climate simulator, MT-CLIM (Running et al., 1987). Simulation over large, heterogeneous watersheds is facilitated by dividing the landscape into a series of facets or hillslope partitions based on geomorphometric principles. Hillslope partitions capture most of the variance in incident short-wave radiation (Band et al., 1991), which means the partitions can be simulated in parallel.

Catenary variations of topography, soils and vegetation within each hillslope are then incorporated as distributional information within hillslope partitions. The distributional information accounts for the variability of lateral subsurface flow, ET, soil drainage, snow-melt, and canopy photosynthesis (Band et al., 1993).

This paper is concerned with the impact of different approaches to soil landscape characterization on three model outputs: Transpiration, canopy net photosynthesis (PSN) and stream flow. Canopy transpiration (mm day^{-1}) is calculated daily using the Penman–Monteith combination equation (Monteith, 1965)

$$\lambda E = \frac{\Delta R_c + \rho_a C_p (D/r_a)}{\Delta + \gamma(1 + (r_c/r_a))} \tag{1}$$

where R_c is net canopy absorbed radiation (W m^{-2}), Δ the slope of the saturation vapor pressure–temperature curve (mb $°C^{-1}$), $\rho_a C_p$ (J m^{-3} $°C^{-1}$) the specific heat density of air, D (mb) the vapor pressure deficit, r_a (s m^{-1}) the bulk aerodynamic resistance for latent heat transfer between the vegetation canopy and its surrounding atmosphere, γ (mb $°C^{-1}$) the psychrometric constant, and r_c (s m^{-1}) is the canopy total stomatal resistance. Canopy resistance is the reciprocal of canopy conductance, which is calculated as the product of LAI and average leaf level stomatal conductance. Stomatal conductance is controlled by light level, air temperature, soil moisture, and vapor pressure deficit (Jarvis, 1976; Lohammar et al., 1980). Gross canopy photosynthesis (kg C m^{-2} day^{-1}) is computed with the CO_2 diffusion gradient, radiation and temperature controlled mesophyll CO_2 conductance, the canopy water vapor conductance, LAI and day-length (Lohammar et al., 1980). Night canopy respiration is computed from night average temperature and foliar biomass. Maintenance respiration for stem and root is computed from biomass and daily average air and soil temperature. Total maintenance respiration is subtracted from gross canopy photosynthesis to give net canopy photosynthesis (PSN).

TOPMODEL accounts for lateral water flux and the spatial distribution of saturation soil water deficit (Band, 1993; Band et al., 1993). The approach taken in TOPMODEL is considered to be 'quasi-distributed' and the watershed is modeled as a distribution of points or elements that are paramized by a hydrological similarity index, W, based on local topography

and soil hydraulic properties

$$W_i = \ln\left(\frac{aT_e}{T_i \tan \beta_i}\right) \tag{2}$$

where a is the upslope contributing area (m^2), T_e the areal averaged transmissivity (m^{-2} day^{-1}), T_i the saturated transmissivity of the local soil, and β_i is the local surface gradient. Saturation soil zone, in the form of a local soil profile saturation deficit, is computed as

$$S_i = \bar{S} + m(\lambda - W)_i \tag{3}$$

where S_i is the local soil profile saturation deficit, measured as a depth below full soil profile saturation (m). $S_i = 0$ where a soil column is fully saturated. $\bar{S}$ is the hillslope or catchment mean saturation deficit and is updated daily on the basis of computed ET, overland flow, base flow, and recharge to the saturated zone from the unsaturated zone. The precipitation (rain or snowmelt) that is not intercepted by canopy or litter is routed to the unsaturated zone. m is a parameter used to describe the rate of exponential decline in saturated hydraulic conductivity with depth in the soil. λ is given as

$$\lambda = \int_a \ln\left(\frac{aT_e}{T_i \tan \beta_i}\right) da \tag{4}$$

Stream flow consists of return flow (for areas when $S_i < 0$), direct precipitation runoff from saturated areas of the basin, and base flow which is computed on a hillslope basis as

$$q_b = T_e \exp(-\lambda) \exp\left(-\frac{\bar{S}}{m}\right) \tag{5}$$

Two key soil properties are needed in RHESSys: rooting zone depth and soil saturated hydraulic conductivity (K_0). In this illustration, we use depth to the bottom of B-horizon (solum depth) as a surrogate for rooting zone depth. Although the effective zone of vegetation water uptake may very well extend beyond the B-horizon into C, fully describing rooting zone depth across landscape can be extremely difficult, if not impossible. The B-horizon provides an initial hypothesis about the spatial variation in rooting depths, even if we are unable to test it at this point. Soil saturated hydraulic conductivity (K_0) is approximated by soil texture based on Van Genuchten (1980)
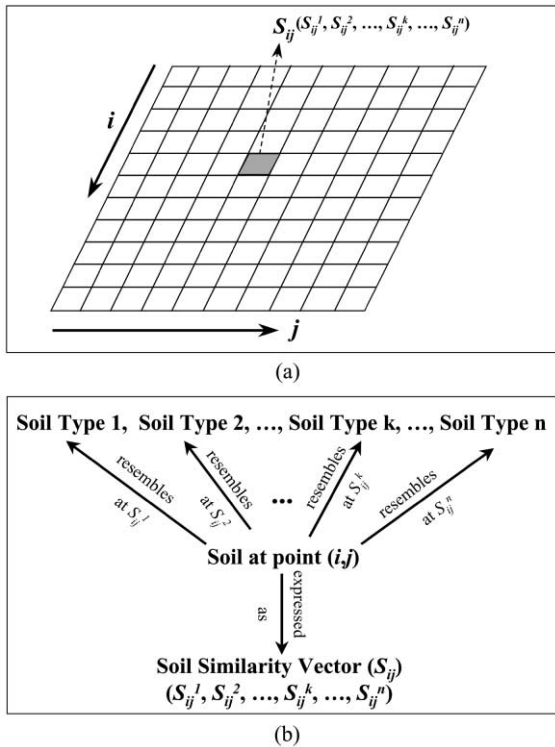
(a)

(b)

Fig. 5. The similarity model in SoLIM: an area is represented as a raster data layer (a) and the soil at each pixel is represented as a similarity vector (b).

and parameterized using the analysis of Rawls et al. (1992). Finally, capillary rise is calculated using a steady-state solution of the Richards Equation (Gardner, 1958).

2.3. Soil landscape paramizations

2.3.1. The two approaches to soil landscape paramization

The soil landscape over the study area was characterized using two different schemes in this study. In the first scheme we derived the spatial distribution of the needed soil properties from a conventional soil map. Each soil polygon was assigned the typical soil property value of its respective assigned soil class. For example, if a soil polygon was labeled as Soil Type One whose typical solum depth value was 100 cm, then the solum depth for the soil in the entire polygon was assigned the value of 100 cm.

Although very few soil polygons are labeled as single class, property values of minor soil types that are expected to be included in a given soil polygon cannot be utilized in a spatially explicit way since the spatial distribution of these inclusions is unknown. Even if the polygon is labeled as a single class polygon, assigning the typical soil property value may not be appropriate since the value of a given soil property varies within a single soil class. Again, because we do not know how the soil property value varies within the polygon we cannot properly use this range of soil property values when deriving the spatial distribution of a given soil property from a conventional soil map. It might be possible to use a Monte Carlo techniques to produce soil property data layer realizations by using the range information in soil description. However, such a soil property data layer would exhibit an unrealistic 'salt and pepper' pattern without the inclusion of spatial autocorrelation in the Monte Carlo analysis. However, information on the spatial autocorrelation of soil properties is often not reported in the soil description and acquiring such information requires a large amount of field data. As a result, only the typical (mode or mean) property value is often used when a conventional soil survey map is used to provide GIS data layer of a given soil property.

The second scheme was the SoLIM approach, which consists of three major components: a similarity model for representing soil spatial variation, a set of inference techniques for populating the similarity model, and the soil information represented under the similarity model (Zhu, 1997). Under the similarity model a given area is represented as a raster layer (Fig. 5a). The size of each grid (pixel) in the raster layer is often very small (such as 10 or 30 m on each side) comparing with the minimum mapping size used in conventional soil maps. The soil at a given pixel (i, j) is then represented by an n-element similarity vector, $\mathbf{S}_{ij} = (S_{ij}^1, S_{ij}^2, \ldots S_{ij}^k \ldots S_{ij}^n)$, where n is the number of prescribed soil classes (such as taxonomic units) over the area and S_{ij}^k is the similarity value of the soil at pixel (i, j) to the prescribed soil class k (Fig. 5b). It must be pointed out that S_{ij}^k is not a probability of whether a certain soil class occurs at a location or not. It is an index which measures the similarity between the local soil at (i, j) to soil class k. The more similar a soil is to a prescribed soil class, the
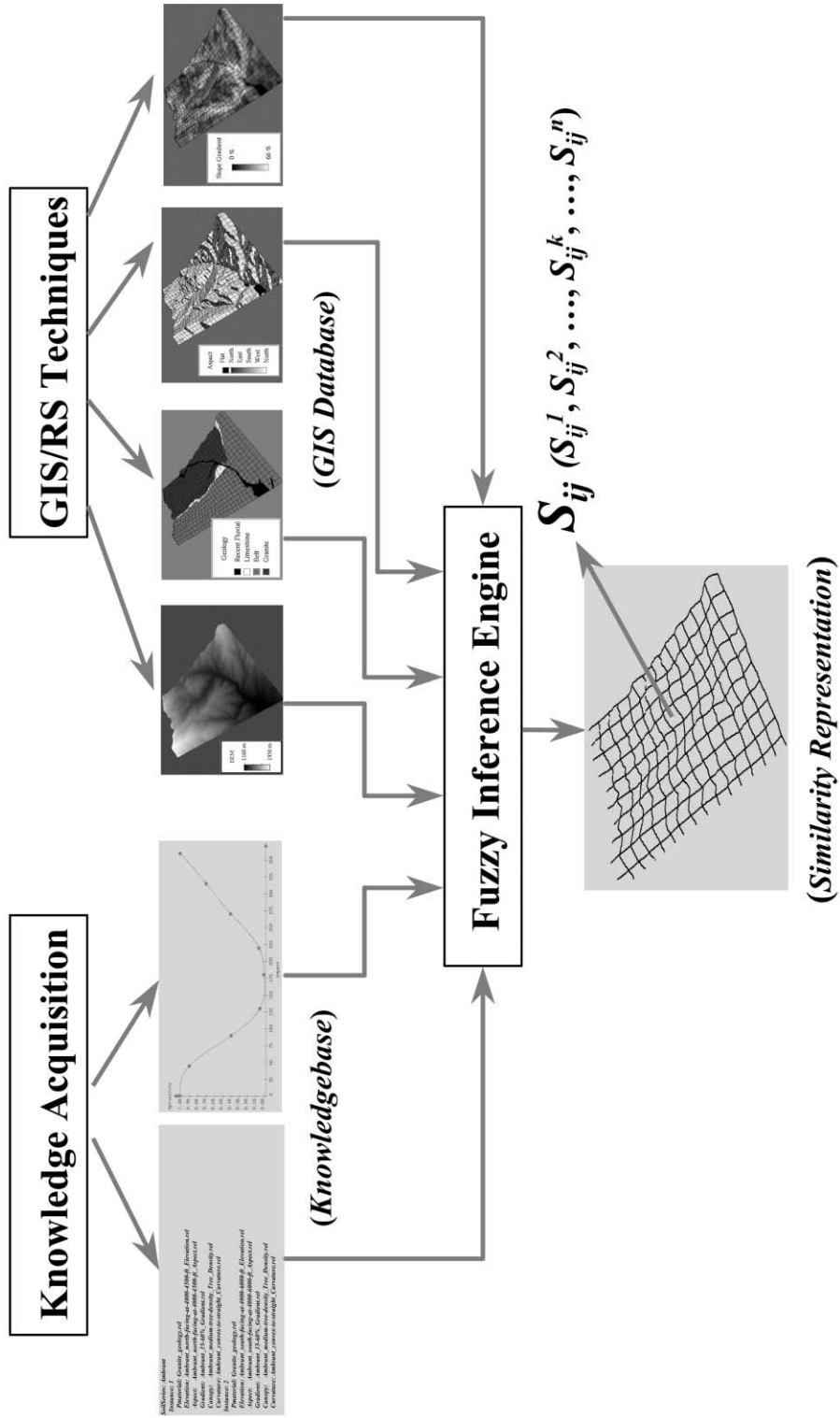
Fig. 6. Populating the similarity model. GIS/RS techniques were used to characterize soil formative environmental conditions and the knowledge acquisition techniques were used to extract knowledge on the relationships between soil and its environmental conditions. A set of inference techniques (the fuzzy inference engine) was used to combine the extracted knowledge with the environmental conditions to determine the similarity of a local soil to a set of prescribed soil classes.
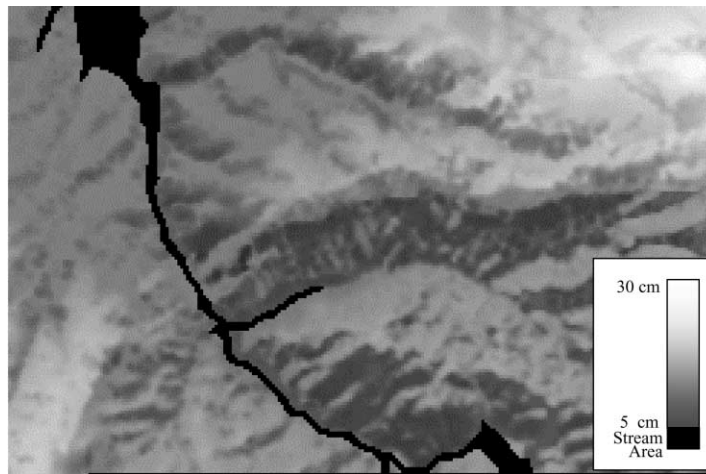
(a)

(b)

Fig. 7. Comparison of *A*-horizon depth inferred using the SoLIM approach (a) with that derived from the conventional soil map (b).

higher its similarity value (fuzzy membership). Thus, a similarity value of 1.0 means that the soil at (i, j) is a typical instance of the prescribed class while a similarity value of 0.0 means that the local soil does not belong to the prescribed soil class at all. With this similarity model spatial variation of soil can be described at the level of pixel size, which is often much smaller than the minimum mapping size of conventional soil maps. As a result, the spatial generalization of soils in conventional soil maps is much reduced under the similarity model. At the attribute level, the soil at a given location is no longer represented by a given class, but rather by a set of similarity values, which allow the intermediate nature of soil to be maintained in this similarity model. The coupling of a raster representation in the spatial domain with a similarity representation in the attribute domain allows the spatial variation of soils to be expressed and retained at much greater details under the similarity model than it can in conventional soil maps.

The SoLIM approach for populating the similarity

model is based on the classic concept that soil is a product of interaction among climatic factors, landform, parent material, organism, and hydrological factors over time (Jenny, 1941; Jenny, 1980; Hudson, 1992). This concept can be expressed in qualitative terms as

$$S = f(\text{Cl}, \text{Og}, \text{Pm}, \text{Tp}, t) \qquad (6)$$

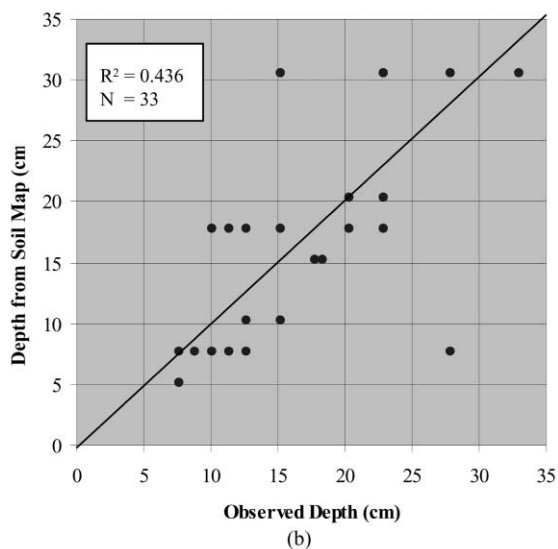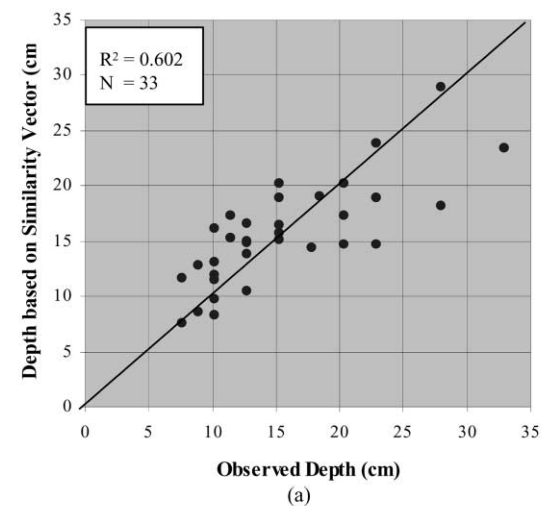where Cl represents climate conditions, Og is for organism, Pm is parent material, Tp stands for

Fig. 8. The scatter plot of depths based on the SoLIM approach vs. observed depths (a) and that of depths from the soil map vs. observed depths (b) at the 33 field sites.

topography, and t is time. We may infer the soil type at a given location if we have local environmental conditions and knowledge of how these environment conditions are related to the soils. Eq. (6) illustrates the general relationship between the soil and its environmental factors. However, the details of the relationship are different at different places. It is very difficult at this stage to derive a mathematical formula for the relationship because of the complexity and limited understanding of both soil forming processes and the paleo-environment. Zhu and Band (1994) and Zhu (2000) approximate the soil-environment relationships and the inference process with the use of artificial intelligence (AI) and GIS/RS techniques (Fig. 6). AI techniques were used to extract knowledge on soil-environment relationships, to give an approximation of f. GIS/RS techniques were used to characterize soil formative environmental conditions (E). The extracted knowledge and the characterized environmental conditions were linked through a set of inference techniques to populate the similarity model for a given area.

The soil information represented under the similarity model can be used to derive spatially continuous soil property maps. Zhu et al. (1997) used the following linear and additive weighting function to estimate A-horizon depths:

$$V_{ij} = \frac{\sum_{k=1}^{n} S_{ij}^k V^k}{\sum_{k=1}^{n} S_{ij}^k} \qquad (7)$$

where V_{ij} is the estimated soil property value at location (i,j), V^k the typical value of a given soil property (e.g. solum depth and hydraulic conductivity) of soil category k, and n is the total number of prescribed soil categories for the area. This function is based on the assumption that, if the local soil formative environment characterized by a GIS resembles the environment of a given soil category, then the property values of the local soil should resemble the property values of the candidate soil category. The resemblance between the environment for soil at (i,j) and the environment for soil category k is expressed as S_{ij}^k, which is used as an index to measure the level of resemblance between
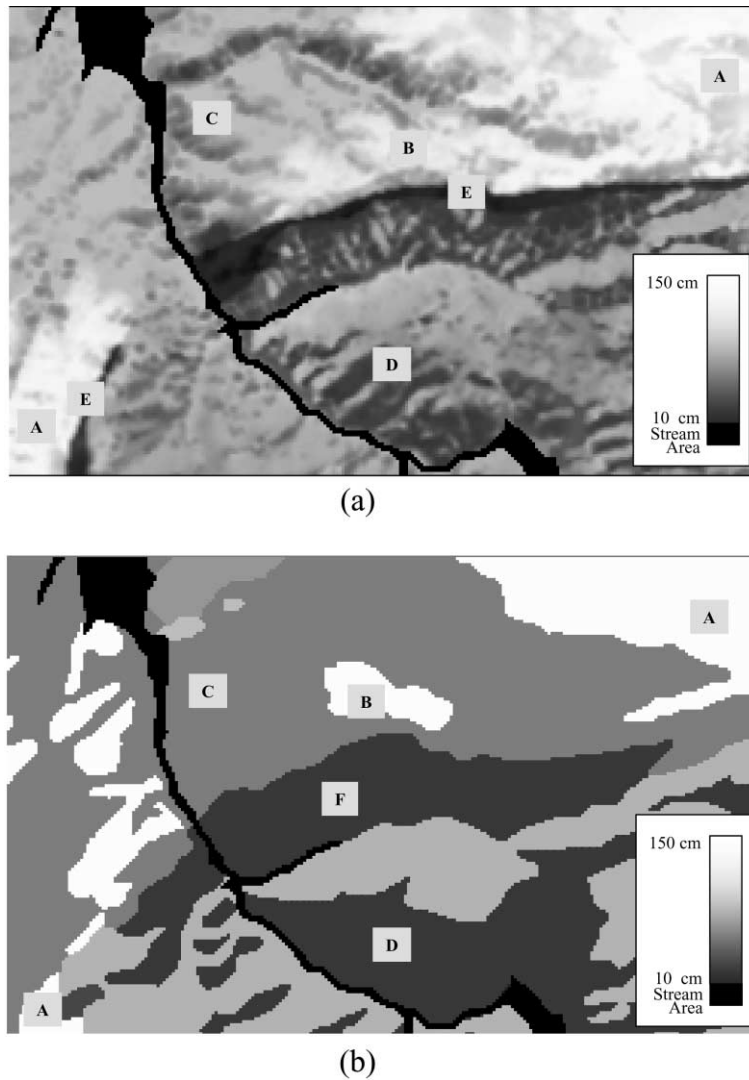
(a)

(b)

Fig. 9. Images of solum depth using two different approaches (light tone means deep solum): (a) using the SoLIM approach; (b) based on the conventional soil map.

the soil property values of the local soil and those of soil category k.

Zhu et al. (1997) reported that the spatial variation of inferred A-horizon depths is more realistic and continuous than that from the conventional soil map (Fig. 7). At 33 field sites the inferred A-horizon depths matched the field observed depths better than the depths derived from the soil map (Fig. 8). They concluded from the case study that the spatial variation of A-horizon depths was better captured in the

inferred depth image than in the depth image derived from the soil map.

2.3.2. Solum depth and hydraulic conductivity data sets

The spatial distributions of solum depth derived from these two schemes (the conventional soil map and the SoLIM approach) are shown in Fig. 9. Fig. 9a shows the spatial variation of solum depth derived from the SoLIM approach and Fig. 9b depicts the
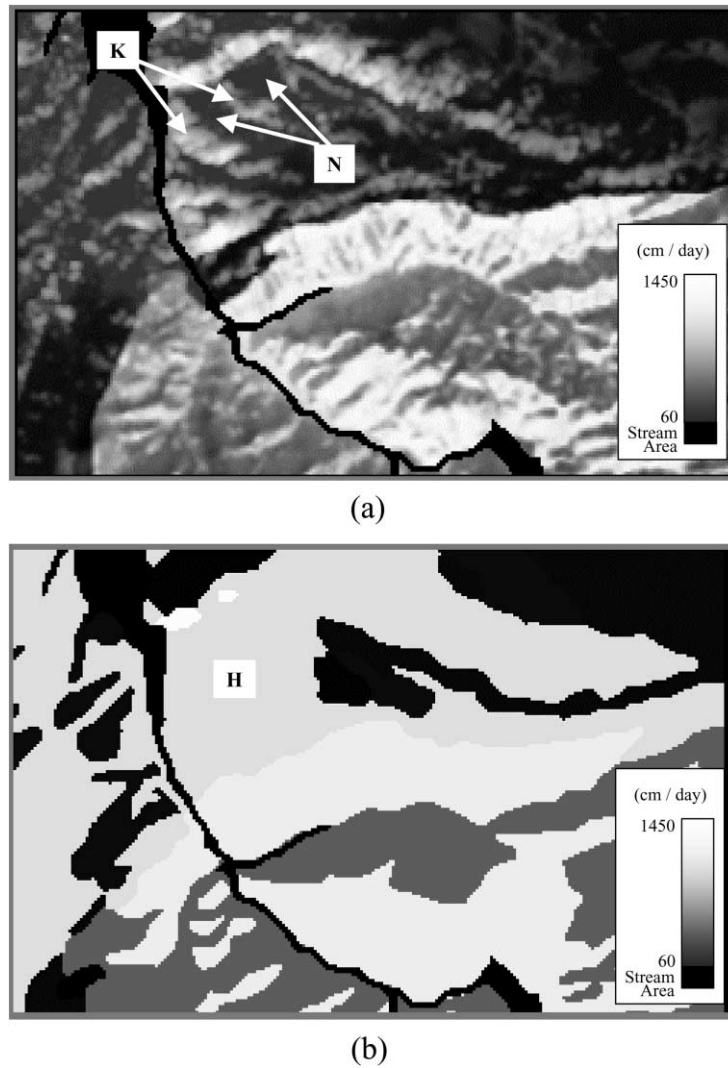
(a)

(b)

Fig. 10. Images of hydraulic conductivity over the study area based on the different approaches (light tone means high conductivity): (a) based on the SoLIM approach; (b) derived from the conventional soil map.

distribution of solum depth based on the conventional soil map. Both images show a similar pattern, which is that solum is deep at high elevation (A) and on north facing slopes (B), and is shallow at low elevation (C) and on south facing slopes (D). However, the differences between the two images are quite strong. First, Fig. 9a shows a gradual variation of solum depth while Fig. 9b depicts sharp changes at the boundaries of soil polygons. Although these sharp changes are possible at locations where major geological material changes (such as areas labeled as E), often these sharp

changes are not realistic and are the artifact of the polygon-based approach in soil mapping. The second difference is that the solum depth from the SoLIM approach reveals much greater details of spatial variation than that from the soil map. For example, the area labeled as F on Fig. 9b shows a homogeneous solum depth. In reality, there are numerous small draws and side-slopes along the major south-facing slope (as shown in Fig. 2a). It is expected that the soil formative environmental conditions on these small draws and side-slopes are different from the major south-facing
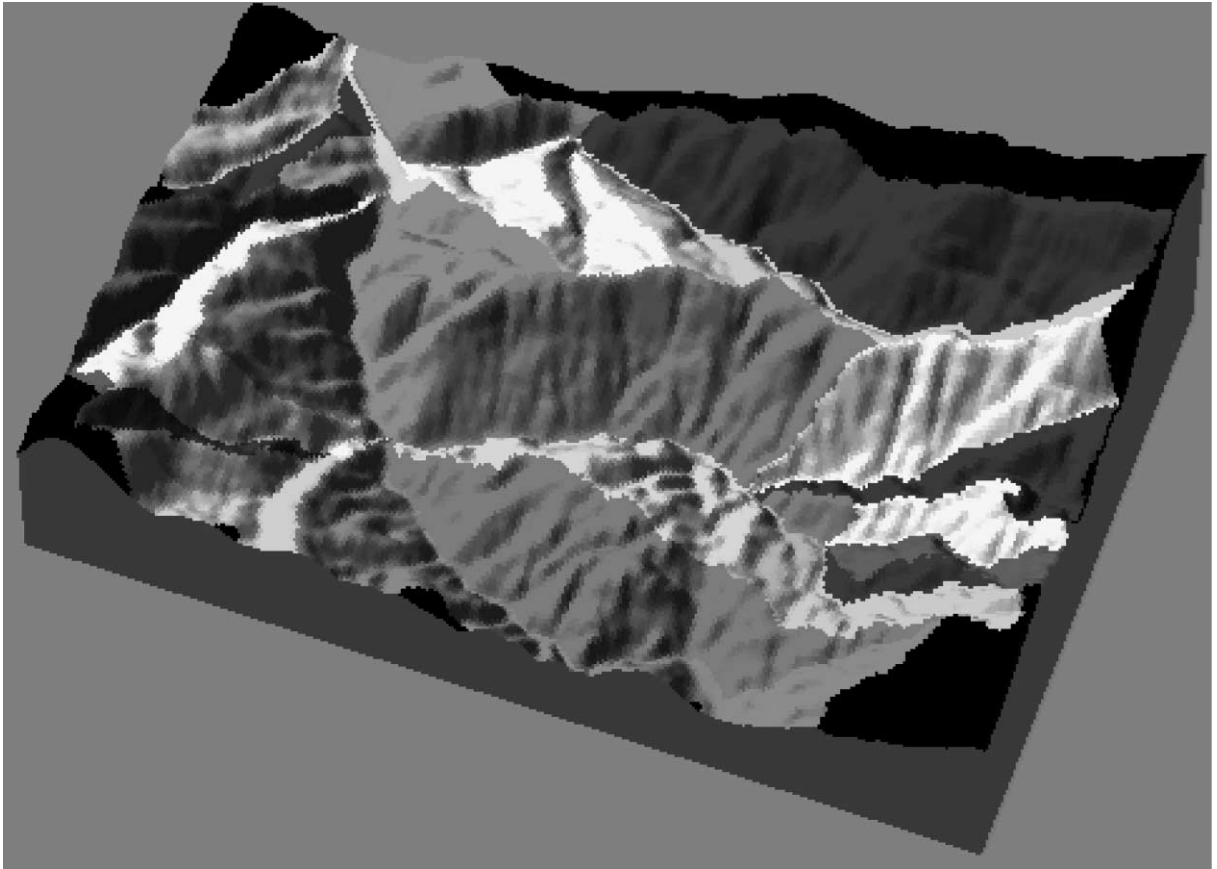
Fig. 11. Hillslope partitions of the Lubrecht area (black areas are not included in this study).

slope and thus the soil profile development would be different. As a result, the solum depth on these draws and side-slopes is expected to be different from that on the major south-facing slope. Therefore, the homogeneous solum depth shown in Fig. 9b is not a good representation of the reality. On the other hand, the solum depth derived from the SoLIM approach depicts detailed spatial variation of solum depth over this major south-facing slope and we expect that the SoLIM derived solum depth would be a more realistic representation of the soil landscape in the area than that from the soil map.

The spatial variation of solum depth portrayed in the solum depth image derived from SoLIM (Fig. 9a) exhibits a similar spatial pattern of A-horizon depth depicted in the A-horizon depth image from SoLIM (Fig. 7a). This can be understood that there is limited human impact in the area and that soil profile

development is largely controlled by local topography and major bedrock materials. Areas that have deeper A-horizons would also have deeper B-horizons. As a result, the spatial variation of solum depth follows the spatial variation of A-horizon depth. Thus, we expect the solum depth image from SoLIM portrays the spatial variation of solum depth in the area better than that from the conventional soil map.

Saturated hydraulic conductivity (K_0) for each of the 12 soil series is approximated by soil texture according to Rawls et al. (1992) and computed for the whole soil profile. Although soil structure, including macropores, plays an important role in the hydraulic properties of soils, in this study we did not consider soil structure in determining hydraulic conductivity since we currently do not have information on how specifically soil structure affects the hydraulic behavior. However, TOPMODEL assumes

Table 4
RHESSys distribution file for Hillslope 21 for the lumped param approach. Only one elevation band and one wetness interval is allowed

Hillslope ID	(# of Elevation bands in the hillslope)					
21	1					

Band	Mean elevation in the band			Number of wetness intervals in the band		
1	1403.69			1		

Wetness Interval ID	Mean Wetness	Area (ha)	LAI (m^2m^{-2})	Ground Coverage	K_O (cm day^{-1})	Rooting Zone Depth (cm)
1	6.59	282.06	12.10	77.5	1387.8	44.6

an exponential decline in saturated hydraulic conductivity with depth through the soil profile, as a result of macroporosity (Beven and Kirkby, 1979), and so this decline is also explicitly modeled in RHESSys.

The spatial distributions of saturated hydraulic conductivity parameterized using the two schemes are shown in Fig. 10. Fig. 10a shows hydraulic conductivity based on the SoLIM approach and Fig. 10b shows that based on the conventional soil map. In general, the soil hydraulic conductivity is high on the granite materials and low on the Belt and limestone materials (see Fig. 2b for bedrock distribution). Hydraulic conductivity also shows contrasts between north and south facing slopes, and between high and low elevations due to the level of soil profile development. It is high on south facing slopes and at low elevations where soil profile development is weak and the accumulation of fine particles in the sub soil horizon is less. On the other hand, the accumulation of fine particles in the sub soil horizon is much stronger on north-facing slopes and at high elevations. As a result, the soil hydraulic conductivity in soils on north-facing slopes and at high elevations is often low. Both Fig. 10a and b show this general pattern. However, Fig. 10a portrays much greater detailed spatial variation of hydraulic conductivity within each major slope area. For example, Fig. 10b shows the hydraulic conductivity to be the same over the major north-facing slope (area labeled as H). On the other hand, Fig. 10a depicts the hydraulic conductivity over the same area to be heterogeneous. Hydraulic conductivity is portrayed in Fig. 10a to be higher for areas with a south facing exposure (labeled as K) than that for areas with a northern exposure or along small draws (labeled as N). This contrast in hydraulic conductivity between the areas with different exposures and at different landform positions is

expected since for this semi-arid to semi-humid region the moisture conditions for areas with a southern exposure are poor and thus soil profile development is very limited. As a result, the soil profiles over these areas consist mostly of coarse materials and hydraulic conductivity is high. On the other hand, higher moisture conditions persist in areas with a northern exposure or in concave areas of the landscape, and so the soil profile development is better in these areas. These soils often have a fine-textured sub horizon and the hydraulic conductivity of soils in these areas is lower than that over areas with a southern exposure. Thus, we expect that the detailed variation of hydraulic conductivity over the landscape depicted in Fig. 10a approximate the spatial variation of hydraulic conductivity better than that derived from the conventional soil map.

2.4. Experiment design

The impacts of the aforementioned differences in soil landscape paramizations on hydro-ecological modeling are examined in the following two ways. First, we examine the impacts on the modeling of overall hydro-ecological responses over an entire area. The overall responses are simulated using two different approaches: The lumped parameter approach and the distributed parameter approach (Maidment, 1993). For both approaches the area was first partitioned into a number of hillslopes (Fig. 11) using the hillslope partition algorithm described in Band (1989). The difference between the two approaches is how information is organized for each hillslope. For the lumped parameter approach, only the mean conditions of model parameters for each hillslope are represented, but no information on their variations within the hillslope is retained. This is accomplished
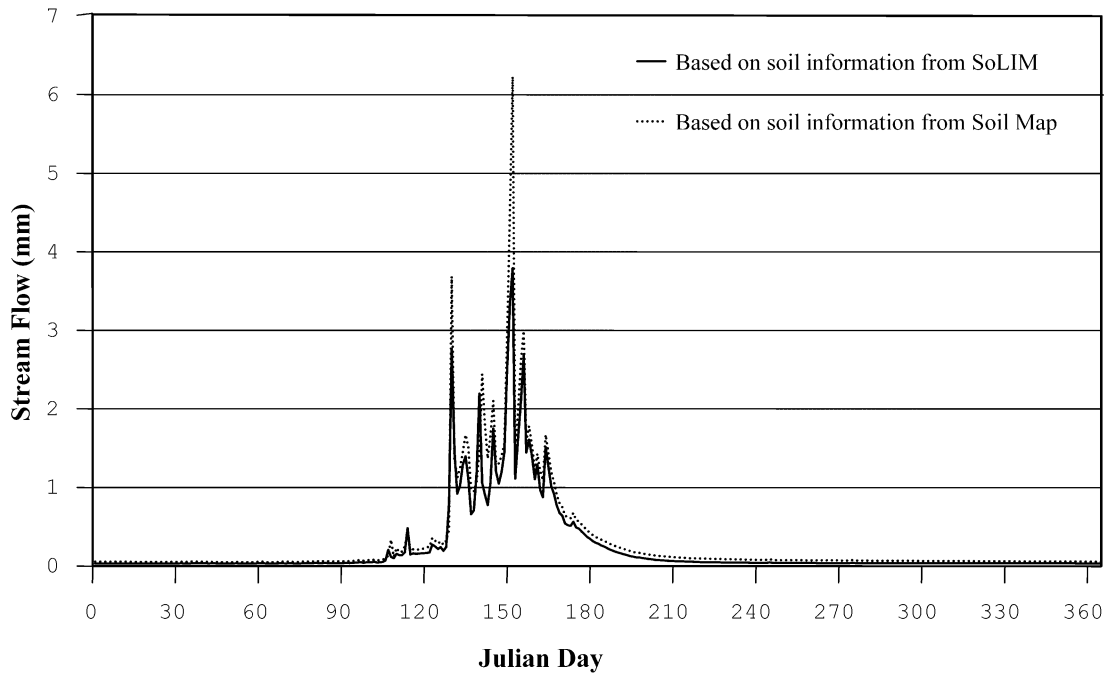
Fig. 12. Comparison of stream flows simulated with RHESSys for the whole watershed using the lumped parameter approach.

under RHESSys by allowing only one elevation band and one wetness interval within each hillslope (Table 4).

For the distributed parameter approach, each hillslope was divided into elevation zones with each zone extending 100 m of elevation. Each elevation zone (band) was further divided into wetness, W_i, intervals using increment sizes of two (Table 3). This way of parameterization allows for the representation of the co-variation of model params within each hillslope.

For each modeling approach, two sets of model parameter files were generated. The two sets only differ from each other in how information on solum depth and hydraulic conductivity were obtained. For one set, the soil information was derived from the conventional soil map of the area. For the other, the soil information was derived from the SoLIM approach using the methodology described in Section 2.3.

The second way of examining the impact of detailed soil spatial variation is to investigate the differences in the spatial distribution of modeled hydro-ecological responses (ET and PSN) across the study area. This was achieved by running RHESSys under the distributed parameter approach outlined

above and by mapping modeled responses across the study area.

3. Results and discussions

3.1. Impacts on modeling overall hydro-ecological responses

3.1.1. Lumped parameter approach

The simulated stream flows from the watershed using the lumped parameter approach are shown in Fig. 12. Under the lumped parameter approach both simulated stream flows fluctuate dramatically with response to rain and snow melt events. This fluctuation can be explained by the fact that the lumped hillslope contributes runoff only when it is fully saturated. However, the stream flow based on the soil information from SoLIM fluctuates much less than that based on the conventional soil map.

The difference in fluctuation of stream flows can be explained by the improved spatial co-variation of soil properties and other landscape variables. The soils in both the spatial and attribute domains are highly
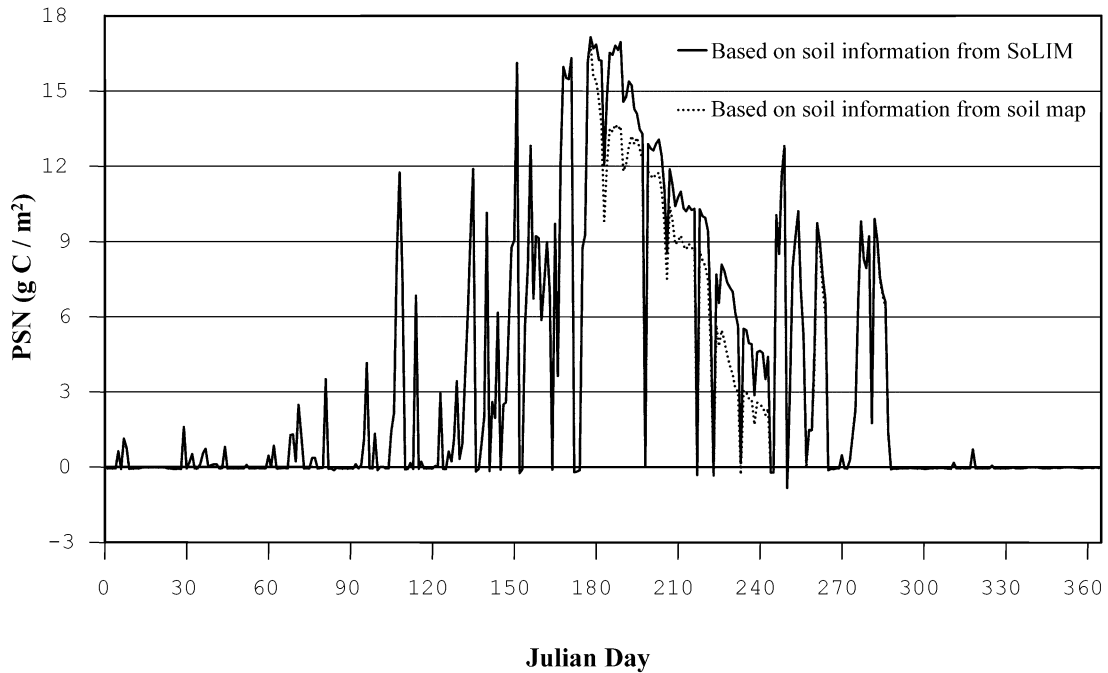
Fig. 13. Comparison of PSN simulated with RHESSys for the whole watershed using the lumped parameter approach.

generalized under the conventional soil mapping approach, but are less generalized with SoLIM. Under the conventional soil mapping approach, different and small soil bodies over a major slope are often mapped as inclusions of a soil polygon for the slope. The characteristics of these smaller soil bodies are often not considered when the soil map is used to characterize the soil landscape for hydro-ecological models. The omission of these smaller soil bodies can over- or under-estimate the hillslope mean soil property values. This is particularly apparent in semi-arid climatic regions where there are large extremes in radiation interception and soil water availability. For instance, in our study area the inclusions on a major south-facing slope are often east- and west-facing side slopes where moisture conditions are wetter due to their topographic concavity and lower potential ET. These conditions favor soil profile development, which in turn leads to deeper solum depth. In addition, soil profile development in our study area means the accumulation of finer particles in the sub soil horizons since the bedrocks in this area produce very coarse textured materials. Thus, the texture of soils on these side

slopes is typical finer than that on the major south-facing slope, and the hydraulic conductivity is lower on these side slopes. These differences in soil properties are not incorporated into the mean under the conventional soil mapping, but are included in the SoLIM approach.

In addition, there can be significant deviation in soil properties from the typical values for the dominant class for an area due to the continuous gradation of exposure. For example, the dominant soil class for a major south-facing slope will best represent the soils for the purely south-facing slopes. As we move away from purely south-facing slopes to other aspects this dominant class may not reflect the changes in soils over the area. If we use the property associated with the dominant class to represent the soils in the entire polygon, then the solum depths will be under-estimated and hydraulic conductivity will be over-estimated. Alternatively, SoLIM uses the similarity model to accommodate this deviation, thus local soil conditions are included in the estimate of the mean.

Underestimation of solum depth results in a soil profile that can be saturated with less amount of precipitation and overestimation of hydraulic
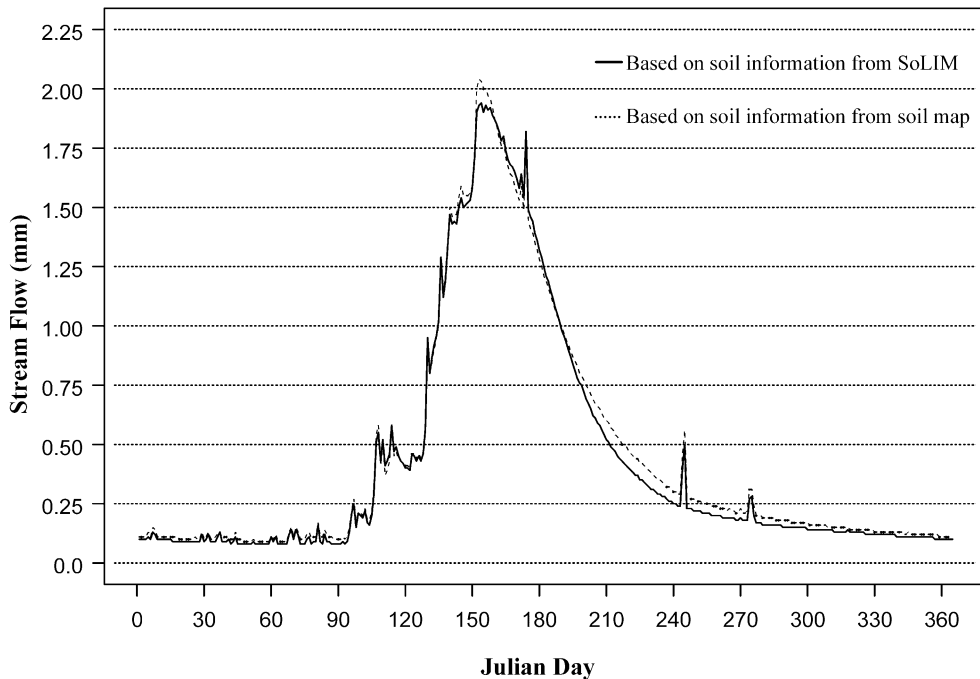
Fig. 14. Comparison of stream flows simulated with RHESSys for the whole watershed using the distributed parameter approach.

conductivity means that the water can move through the soil column more quickly. Thus soils respond more quickly and abruptly to precipitation events and produce a highly fluctuated hydrograph (Fig. 12). Due to the improved representation of soil-landscape under the SoLIM scheme, the soil conditions on the side slopes and their deviation from the dominant type are considered in the model paramization. As a result, the peaks of the simulated hydrograph are lower.

Annual variations of net photosynthesis (PSN) simulated using the lumped parameter model are shown Fig. 13. PSN is not influenced by soil parameter variability during the first five and half months of the year. However, it starts to differ towards later part of June and the difference continues throughout the summer into early September, after which simulated PSN become the same again.

The three episodes coincide with the three periods of climatic conditions for the area (Fig. 3). The year starts for the area with low temperature and low precipitation (mostly in the form of snow). As the year progresses, the temperature and precipitation increases. With higher temperatures snow starts to

melt. As a result, soil water contents are high. There is no moisture stress for the area. When the area enters early summer (later June), the temperature still increases but the amount of precipitation decreases. By that time the snow has melted, and subsequent soil water recharge is limited to infrequent rainfall events. However, during summer months there is a soil water draw down via ET. Eventually, the area experiences moisture stress and photosynthetic activities reduces. By the end of summer temperature decreases and the amount of precipitation increases. Soil water contents increase and moisture stress dissipates.

The simulated PSN differs between the two soil paramization schemes during the period of moisture stress when stomatal closure occurs. It is understandable that during the time when recharge to soil water equals or surpasses soil water depletion the amount of available water stored in soil profile is not important. However, the ability of storing water in a soil profile (a function of soil water holding capacity and solum depth) becomes very critical when soil water depletion is faster than recharge since plants draw water from soil storage. As time goes on soil water over
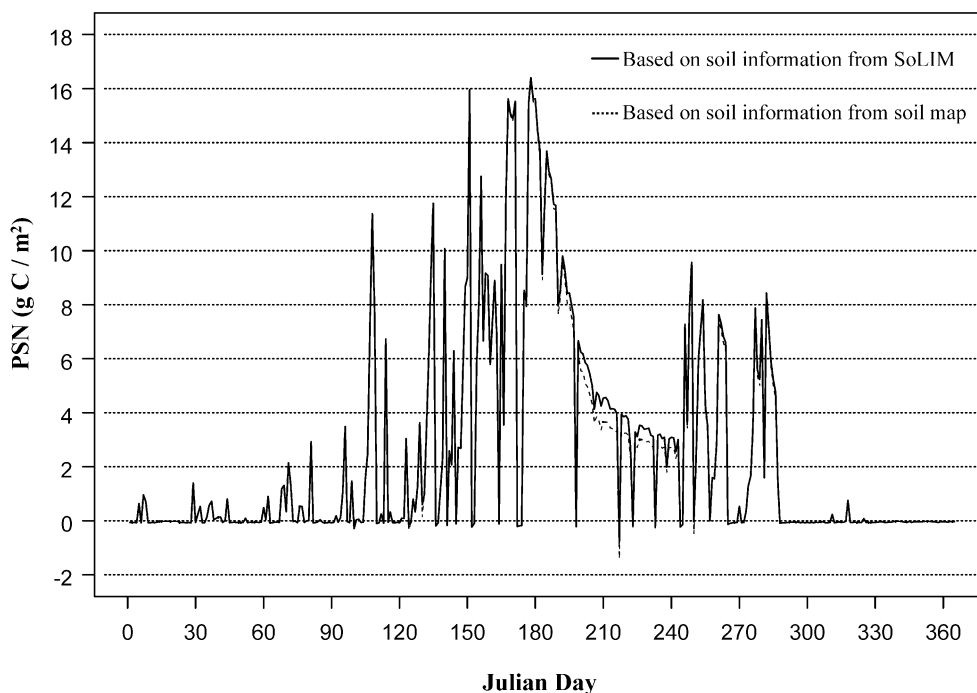
Fig. 15. Comparison of PSN simulated with RHESSys for the whole watershed using the distributed parameter approach.

areas with lower soil water storage will be depleted faster and moisture stress shows up earlier and is more severe. As a result, PSN will be further reduced. Fig. 13 shows that the PSN simulated based on the soil information from the conventional soil map is much lower over the period of moisture stress than that simulated using the information from SoLIM. This can be explained with reference to the earlier discussion that the conventional soil map typically under-estimates solum depth and overestimates hydraulic conductivity on south facing slopes. Since south facing slopes dry faster than north facing slopes due to higher radiation interception, the soil water storage in the soils over these south facing slopes are lower based on the soil map and the moisture stress shows up earlier and more severe than that based on SoLIM (Fig. 13).

3.1.2. Distributed parameter approach

Stream flow and PSN simulated using the distributed approach are shown in Figs. 14 and 15. The stream flow hydrographs are very different from those from the lumped parameter approach (Fig. 12)

due to the fact the distributed approach not only considers the mean conditions, but also incorporates spatial variation within each hillslope. Under a distributed framework surface runoff generation occurs over a partial contributing area, as opposed to all or none of the hillslope area in the lumped parameter approach. The detailed comparison and discussion on the differences between the lumped versus distributed approaches can be found in Band et al. (1993) and are out of the scope of this study. However, what we want to discuss is the difference in the impacts of different soil landscape paramization strategies on the lumped and distributed modeling approaches. The difference between the two hydrographs under the distributed approach is small compared to that under the lumped parameter approach. This is due to the fact the distributed approach considers the spatial co-variation of local topography (elevation and slope gradient) and drainage area within a given hillslope. Thus, much of local variation of soil properties (such as solum depth and hydraulic conductivity) is expressed by this detailed description of other landscape parameters. As a result the difference
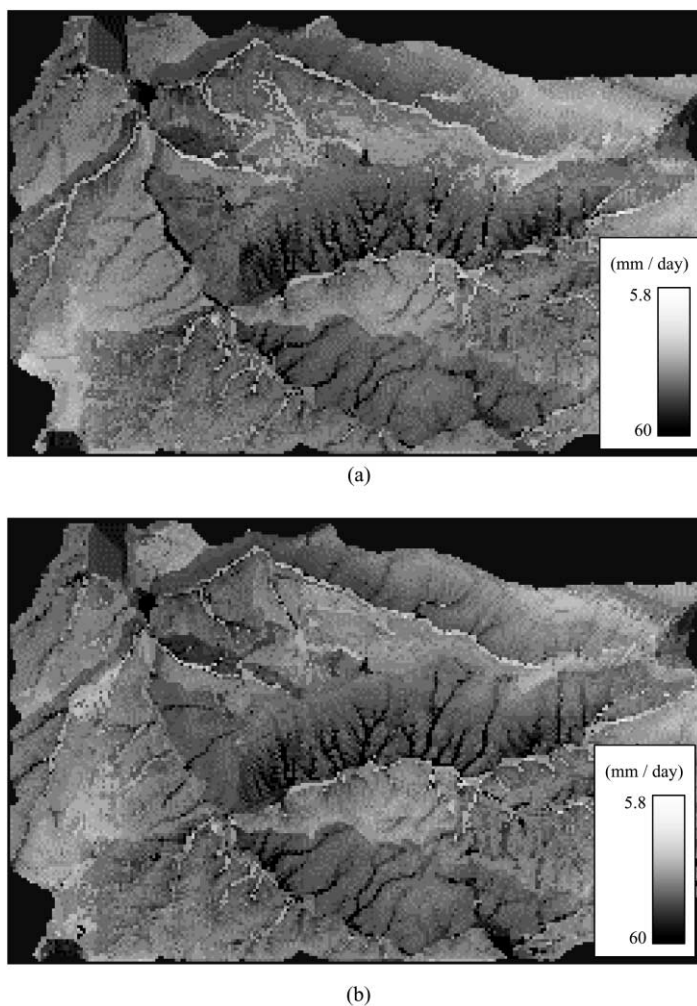
(a)

(b)

Fig. 16. Spatial distributions of transpiration simulated from RHESSys for year day 181 when there is no moisture stress over the area: (a) based on the soil information derived from SoLIM; (b) based on soil information from the soil map.

in simulated stream flow between the two different soil landscape parametrization schemes is small under the distributed approach.

PSN simulated under the distributed approach exhibits similar temporal pattern as discussed in Section 3.1.1 (Fig. 15). However, the difference in PSN between the two different soil landscape parameterization schemes is again much smaller. In particular, the difference in PSN between the two schemes starts much later in the growing season (Fig. 15). This can be explained by the fact that the representation of spatial co-variation of local topography and drainage area under the distributed approach captures the major

variation of local soil conditions, and the impacts of over- or under-estimation of soil properties in the conventional soil map are much reduced under the distributed approach.

3.2. Impacts on modeling the spatial variation of hydro-ecological responses

Spatial distributions of the simulated transpiration under the different soil landscape paramization schemes are shown in Figs. 16 and 17. We are not showing spatial distributions of PSN, as it is explained by the same limiting factor (i.e. stomatal conductance)
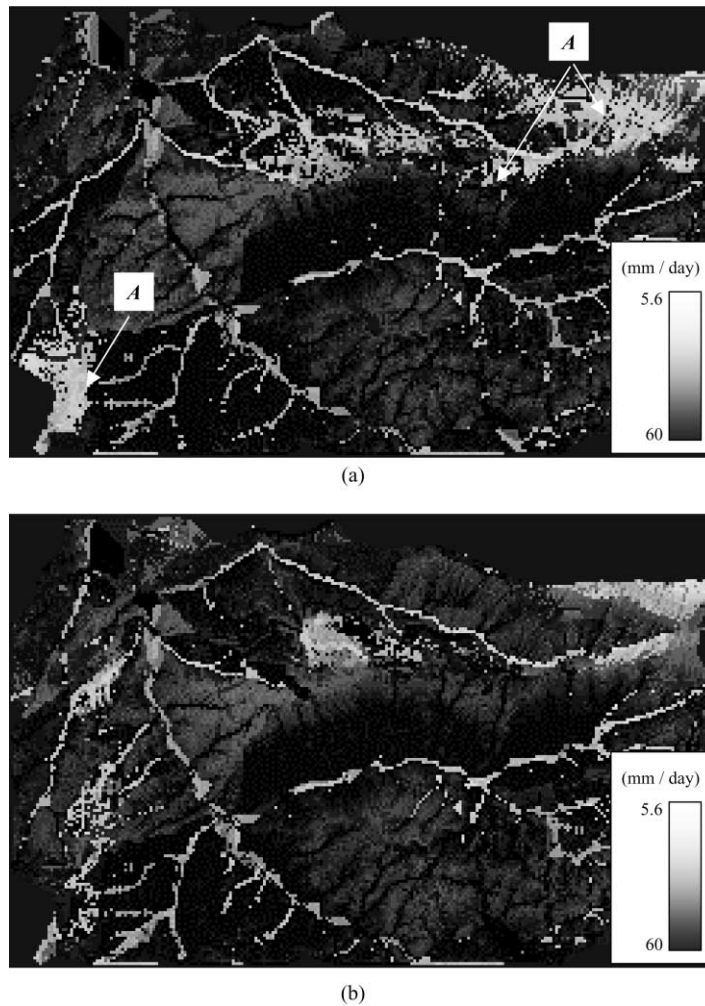
(a)

(b)

Fig. 17. Spatial distributions of transpiration simulated from RHESSys for year date 200 when there is a moisture stress over the area: (a) based on the soil information derived from SoLIM; (b) based on soil information from the soil map.

as ET in this highly water-limited environment. Fig. 16 shows the spatial distributions of the simulated transpiration for year day 181. The differences between the two images (Fig. 16a and b) are very subtle. This means that the detailed soil paramization from SoLIM has no significant impact on the spatial distribution of the simulated transpiration for that day. This can be explained by the fact that during that period of time moisture stress has not yet occurred (Fig. 3), and the amount of available water stored in soil profiles has not yet played an important role in sustaining ecological responses. Thus, the impact of detailed description of local variation of solum depth

and hydraulic conductivity on soil water content cannot be reflected in the ecological process. However, on year day 200 when the area is experiencing severe moisture stress the spatial distributions of simulated transpiration is different (Fig. 17a and b), particularly areas over major south facing slopes (Area A) where solum depth is underestimated. This is due to the fact that the amount of transpiration is now largely dependent on the amount of available water stored in the soil profiles. The impact of underestimating solum depth and over-estimating soil hydraulic conductivities on soil moisture content over these south facing slopes is now manifested in

the spatial distribution of simulated ecological processes.

4. Conclusions

This study reveals that the detailed soil landscape paramization using the SoLIM scheme has significant impacts on the simulated hydro-ecological processes with the lumped parameter approach. The peak stream flows were reduced when using SoLIM in comparison to the flows based on the soil information from a conventional soil map. The detailed soil information from SoLIM does not have much impact on the simulation of PSN over the period when there is a sufficient water recharge to soil profiles. However, the simulated PSN production based on the detailed soil information is higher over the moisture stress period than that based on the soil information from the conventional soil map.

With the distributed parameter approach the detailed soil spatial information derived from the SoLIM scheme has much less impact on the simulation of hydro-ecological processes. The simulated hydrograph based on detailed soil information is very similar to that based on the soil information from the soil map. The difference in simulated PSN production during the period of moisture stress is smaller between the two different soil landscape parameterizations and this difference also occurred much later in the moisture stress period than it was under the lumped parameter approach. The impacts of detailed soil parameterization on spatial distribution of simulated transpiration occurred mainly over south facing slopes during the period of moisture stress.

These findings imply that distributed parameter models applied in mountainous watersheds may account for a large portion of the co-variation in soil properties since soil development and hydrologic fluxes are both dominated by topography in these environments. This suggests that, at least for short-term hydrologic simulations, topographically dominated systems with adequate plant available water may be simulated with conventional soil maps using a distributed approach. We note that small differences in timing of moisture stress may have cumulative effects on the simulated productivity of forest eco-systems. For inter-annual or longer simulations the cumulative effects on productivity may lead to differences in forest growth and over time forest water use.

Acknowledgements

References

Band, L.E., 1989. A terrain based watershed information system. Hydrological Processes 3, 151–162.

Band, L.E., 1993. Effect of land surface representation on forest water and carbon budgets. Journal of Hydrology 150, 749–772.

Band, L.E., Moore, I.D., 1995. Scale: landscape attributes and geographical information systems. Hydrological Processes 9, 401–422.

Band, L.E., Peterson, D.L., Running, S.W., Coughlan, J., Lammers, R., Dungan, J., Nemani, R., 1991. Forest ecosystem processes at the watershed scale: basis for distributed simulation. Ecological Modeling 56, 171–196.

Band, L.E., Patterson, P., Nemani, R., Running, S.W., 1993. Forest ecosystem processes at the watershed scale: incorporating hill-slope hydrology. Agricultural and Forest Meteorology 63, 93–126.

Beven, K., 1986. Runoff production and flood frequency in catchments of order n: an alternative approach. In: Gupta, V.K. (Ed.). Scale Problems in Hydrology. Reidel, Hingham, p. 107.

Beven, K.J., Kirkby, M.J., 1979. A physically based, variable contributing model of basin hydrology. Hydrological Sciences Bulletin 24, 43–69.

Burrough, P.A., 1996. Opportunities and limitations of GIS-based modeling of solute transport at the regional scale. In: Corwin, D.L., Laogue, K. (Eds.). Applications of GIS to the Modeling of Non-point Source Pollutants in the Vadose Zone. SSSA Special Publication No. 48SSSA, Madison, pp. 19–38.

Corwin, D.L., 1996. GIS applications of deterministic solute transport models for regional-scale assessment of non-point source pollutants in the vadose zone. In: Corwin, D.L., Laogue, K. (Eds.). Applications of GIS to the Modeling of Non-point Source Pollutants in the Vadose Zone. SSSA Special Publication No. 48SSSA, Madison WI, pp. 69–100.

Gardner, W.R., 1958. Some steady-state solutions of the unsaturated moisture flow equations with application to evaporation from a water table. Soil Science 85 (4), 228–232.

Hudson, B.D., 1992. The soil survey as paradigm-based science. Soil Science Society of America Journal 56, 836–841.

Jarvis, P.G., 1976. The interpretation of the variations in leaf water potential and stomatal conductance found in canopies in the

field. Philosophical Transactions of the Royal Society of London, Series B 273, 593–610.

Jenny, H., 1941. Factors of Soil Formation: A System of Quantitative Pedology. McGraw-Hill, New York, p. 281.

Jenny, H., 1980. The Soil Resource: Origin and Behaviour. Springer, New York, p. 377.

Lammers, R.B., Band, L.E., Tague, C.L., 1997. Scaling behaviour of watershed processes. In: van Gardingen, P., Foody, G., Curran, P. (Eds.). Scaling-Up: From Cell to Landscape. Cambridge University Press, Cambridge, pp. 295–317.

Lohammar, T., Larsson, S., Linder, S., Falk, S.O., 1980. FAST — simulation models of gaseous exchange in Scots pine. Ecological Bulletin 32, 505–523.

Luxmoore, R.J., Sharma, M.L., 1980. Runoff responses to soil heterogeneity: experimental and simulation comparisons for two contrasting watershed. Water Resources Research 16 (4), 675–684.

Luxmoore, R.J., Sharma, M.L., 1984. Evapotranspiration and soil heterogeneity. Agricultural Water Management 8, 279–289.

Lytle, D.L., 1993. Digital soils databases for the United States. In: Goodchild, M.F., Parks, B.O., Steyaert, L.T. (Eds.). Environmental Modeling with GIS. Oxford University Press, New York, pp. 386–391.

Maidment, D.R., 1993. GIS and hydrologic modeling. In: Goodchild, M.F., Parks, B.O., Steyaert, L.T. (Eds.). Environmental Modeling with GIS. Oxford University Press, New York, pp. 147–167.

Mackay, D.S., Band, L.E., 1997. Forest ecosystem processes at the watershed scale: dynamic coupling of distributed hydrology and canopy growth. Hydrological Processes 70, 1197–1217.

Miller, E.E., Miller, R.D., 1965. Physical theory for capillary flow phenomena. Journal of Applied Physics 27, 324–332.

Monteith, J.L., 1965. Evaporation and environment. In: Fogg, G.E. (Ed.). The State and Movement of Water in Living Organisms, vol. 19. Academic Press, California, pp. 205–234.

Nemani, R., Pierce, L., Running, S., Band, L.E., 1993. Forest ecosystem processes at the watershed scale: sensitivity to remotely sensed leaf area index estimates. International Journal of Remote Sensing 14, 2519–2534.

Nielsen, R.D., Bigler, R.J., Sobecki, T., Lytle, D.L., 1996. Applications of soil survey attribute data to GIS pollution assessment models. In: Corwin, D.L., Laogue, K. (Eds.). Applications of GIS to the Modeling of Non-point Source Pollutants in the Vadose Zone. SSSA Special Publication No. 48SSSA, Madison WI, pp. 175–183.

Nimlos, J.T., 1986. Soils of Lubrecht Experimental Forest, Miscellaneous Publication No. 44, Montana Forest and Conservation Experiment Station, School of Forestry, University of Montana, Missoula, Montana, 36pp..

Peck, A.J., Luxmoore, R.J., Stolzy, J.L., 1977. Effects of spatial variability of soil hydraulic properties in water budge modeling. Water Resources Research 13 (2), 348–354.

Rawls, W.J., Ahuja, L.R., Brakensiek, D.L., 1992. Estimating soil hydraulic properties from soils data. In: Van Genuchten, M.Th., Liej, F.J. (Eds.). (Indirect Methods for Estimating the Hydraulic Properties of Unsaturated Soils). University of California Press, Riverside, pp. 329–340.

Ross, R.L., Hunter, H.E., 1976. Climax Vegetation of Montana Based on Soils and Climate. USDA Soil Conservation Service, Bozeman, Montana, p. 36.

Running, S.W., Coughlan, J.C., 1988. A general model of forest ecosystem processes for regional applications: I. Hydrologic balance, canopy gas exchange and primary production processes. Ecological Modeling 42, 125–154.

Running, S.W., Gower, S.T., 1991. FOREST-BGC, a general model of forest ecosystem processes for regional applications. II. dynamic carbon allocation and nitrogen budgets. Tree Physiology 9, 147–160.

Running, S.W., Nemani, R.R., Hungerford, R.D., 1987. Extrapolation of synoptic meteorological data in mountainous terrain, and its use for simulating forest evapotranspiration and photosynthesis. Canadian Journal of Forest Research 17, 472–483.

Running, S.W., Nemani, R.R., Peterson, D.L., Band, L.E., Potts, D.F., Pierce, L.L., 1989. Mapping regional forest evapotranspiration and photosynthesis by coupling satellite data with ecosystems simulation. Ecology 70, 1090–1101.

Seyfried, M., 1998. Spatial variability constraints to modeling soil water at different scales. Geoderma 85, 231–254.

Sharma, M.L., Luxmoore, R.J., 1979. Soil spatial variability and its consequences on simulated water balance. Water Resources Research 15 (6), 1567–1573.

Sharma, M.L., Gander, G.A., Hunt, C.G., 1980. Spatial variability of infiltration in a watershed. Journal of Hydrology 45, 101–122.

Sivapalan, M., Beven, K., Wood, E.F., 1987. On hydrologic similarity 2: a scaled model of storm runoff production. Water Resources Research 23 (12), 2266–2278.

Van Genuchten, M.Th., 1980. Predicting the hydraulic conductivity of unsaturated soils. Soil Science Society of America Journal 44, 892–898.

Waring, R.H., Running, S.W., 1998. Forest Ecosystem: Analysis at Multiple Scales. Academic Press, New York.

Zhu, A.X., 1997. A similarity model for representing soil spatial information. Geoderma 77, 217–242.

Zhu, A.X., 1999a. Fuzzy inference of soil patterns: implications for watershed modeling. In: Corwin, D.L., Loague, K., Ellsworth, T.R. (Eds.). Advanced Information Technologies for Assessing Nonpoint Source Pollution in the Vadose Zone. Washington, D.C. Geophysical Monograph 108AGU Publication, pp. 135–149.

Zhu, A.X., 1999b. A personal construct-based knowledge acquisition process for natural resource mapping. International Journal of Geographical Information Science 13, 119–141.

Zhu, A.X., 2000. Mapping soil landscape as spatial continua: the neural network approach. Water Resources Research 36, 663–677.

Zhu, A.X., Band, L.E., 1994. A knowledge-based approach to data integration for soil mapping. Canadian Journal of Remote Sensing 20, 408–418.

Zhu, A.X., Band, L.E., Dutton, B., Nimlos, T.J., 1996. Automated soil inference under fuzzy logic. Ecological Modelling 90, 123–145.

Zhu, A.X., Band, L.E., Vertessy, R., Dutton, B., 1997. Derivation of soil properties using a soil land inference model (SoLIM). Soil Science Society of America Journal 61, 523–533.